Nat. Hazards Earth Syst. Sci., 8, 1009–1017, 2008
www.nat-hazards-earth-syst-sci.net/8/1009/2008/

Natural Hazards and Earth System Sciences

Ionospheric conductivity effects on electrostatic field penetration into the ionosphere

V. V. Denisenko[1,2], **M. Y. Boudjada**[3], **M. Horn**[4], **E. V. Pomozov**[1], **H. K. Biernat**[3,5], **K. Schwingenschuh**[3], **H. Lammer**[3], **G. Prattes**[6], **and E. Cristea**[3]

[1]Institute of Computational Modeling, Russian Academy of Sciences, Siberian Branch, Krasnoyarsk, Russia
[2]Siberian Federal University, Krasnoyarsk, Russia
[3]Space Research Institute, Austrian Academy of Science, Graz, Austria
[4]Institute of Physics, Department of Geophysics, Astrophysics and Meteorology, Karl-Franzens-University Graz, Austria
[5]Institute of Physics, Department of Theoretical Physics, Karl-Franzens-University Graz, Austria
[6]Communication Networks and Satellite Communications Institute, Technical University Graz, Austria

Received: 7 May 2008 – Revised: 18 July 2008 – Accepted: 22 July 2008 – Published: 17 September 2008

Abstract. The classic approach to calculate the electrostatic field penetration, from the Earth's surface into the ionosphere, is to consider the following equation $\nabla\cdot\left(\hat{\sigma}\cdot\nabla\Phi\right)=0$ where $\hat{\sigma}$ and Φ are the electric conductivity and the potential of the electric field, respectively. The penetration characteristics strongly depend on the conductivities of atmosphere and ionosphere. To estimate the electrostatic field penetration up to the orbital height of DEMETER satellite (about 700 km) the role of the ionosphere must be analyzed. It is done with help of a special upper boundary condition for the atmospheric electric field. In this paper, we investigate the influence of the ionospheric conductivity on the electrostatic field penetration from the Earth's surface into the ionosphere.

We show that the magnitude of the ionospheric electric field penetrated from the ground is inverse proportional to the value of the ionospheric Pedersen conductance. So its typical value in day-time is about hundred times less than in night-time.

1 Introduction

First unusual disturbances of the vertical component E_z of the electrostatic field were observed prior to earthquakes in the epicentral zones on the Earth's surface by Kondo (1968). Electrostatic potential fluctuations were measured onboard a satellite at an altitude of 400 km (Kelley and Mozer, 1972). A systematic research started to develop in 80th (Gokhberg et al., 1983). Response of the atmosphere and the ionosphere to intense earthquakes were reported by several studies (Kelley et al., 1985; Kingsley, 1989; Pogorel'tsev, 1989; Depuev and Zelenova, 1996; Ruzhin and Depueva, 1996). Also disturbances related to nuclear accidents were observed (Ruzhin et al., 1995; Martynenko et al., 1996) and associated to the propagation of acoustic-gravity waves (Row, 1967). More details about these investigations and others are reviewed by Parrot (1995).

1.1 Models of seismic precursory phenomena

According to the sources of precursory phenomena, models are generally based on the formation of micro-cracks in the days to weeks before the event (Molchanov and Hayakawa, 1995, 1998). Due to mechanical forces on a specific part of the lithosphere, micro-cracks appear, which increase in their number density and finally end in the earthquake itself. Part of the mechanical energy, which is released due to the cracks, is transformed into electromagnetic energy (Mastov and Lasukov, 1989; Molchanov et al., 1995). The resulting electromagnetic emission is in the same frequency range as the mechanical disturbances and is in the low frequency parts (kHz and below). Since parts of the lithosphere are saturated with water, cracks also result in changes of the pore water pressure, which leads to electrokinetic effects (Gershenzon et al., 1993). Movement of crustal material (e.g. due to seismic waves) may result in inductive effects due to a relative movement in the geomagnetic field. Additionally, the Earth's crust involves piezomagnetic and electric features.

Correspondence to: M. Y. Boudjada
(mohammed.boudjada@oeaw.ac.at)

Published by Copernicus Publications on behalf of the European Geosciences Union.

All these effects or changes in the electromagnetic environment of the near Earth atmosphere due to chemical mechanisms may lead to the rise of electromagnetic fields on the Earth's surface (Gershenzon and Bambakidis, 2001). Several models have been proposed to summarize the main physical mechanisms and the corresponding effects starting from the ground up to the ionosphere/magnetosphere (Gokhberg et al., 1985; Pulinets et al., 2000, 2002; Sorokin et al., 2001; Molchanov et al., 2004). Characteristic variations in the critical frequency foF2 (Silina et al., 2001), the total electron content (Liu et al., 2004), the ion temperature (Sharma et al., 2006) or the local ion and electron density (Parrot et al., 2006) were found.

1.2 Electric field penetration in the ionosphere

In the frame of ionospheric precursors, it is important to know what kind of effect could be observable to maintain proper satellite missions. In this connection it is essential to understand how electrostatic fields from lithospheric origin penetrate into higher altitudes of the atmosphere. Theoretical investigations are generally based on the work of Park and Dejnakarintra (1973). This approach was mainly applied to study the penetration of thundercloud electric field into the ionosphere and the magnetosphere. First this model has been used and developed towards a better description of physical phenomena occurring during lightning (Roble and Hays, 1979; Nisbet, 1983; Makino and Ogawa, 1984; Tsur and Roble, 1985; Baginski et al., 1988; Khegay et al., 1990; Ma et al., 1998; Velinov and Tonov, 1995; Rodger et al., 1998). The conductivity of the atmosphere is found to be a key physical parameters in the processes which occurred between the ground and the other layers, in particular the ionosphere (James, 1985; Kim and Khegay, 1985; Kamra and Ravichandran, 1993). A second application of the model of Park and Dejnakarintra (1973) is discussed and investigated in the frame of the studies of the seismic precursor emissions. In this case the electric field of seismic origin is analyzed in the way to estimate the effect of such field within the ionosphere (Gokhberg et al., 1984; Kim et al., 1994; Pulinets et al., 1998). One has also to report models based on enhancement of radioastivity and charged aerosols in the atmosphere before earthquakes (Pierce, 1976; Boyarchuk et al., 1998; Sorokin et al., 2000, 2005). The general conclusion is that electric fields can effectively penetrate into the ionosphere and disturb the ionospheric plasma under certain circumstances.

The field penetration is more effectively at night and the field intensity value critically depends on the characteristic source dimension, which could be described by the earthquake preparation area (Dobrovolsky et al., 1979). Pulinets et al. (2003) concluded that the electrostatic field effectively penetrates into the ionosphere when the source area is greater than 100 to 200 km. This corresponds to a magnitude greater than 4.6 to 5.3, which is some kind of threshold value for the ionospheric sensibility. Grimalsky et al. (2003) estimated a critical value for the ground electrostatic field of the order of 1 to 3 kV/m. These values were also discussed in the frame of in-situ measurements (Mikhailov et al., 2007).

The effect of a near Earth precursory sign on the ionosphere can be determined by the projection along geomagnetic field lines. In a simplified approach, the inclination of the geomagnetic field lines is taken to be $I=90°$ (which is nearly the case at the geomagnetic poles) and the atmospheric conductivity is assumed to be isotropic. The atmospheric (and ionospheric) conductivity has the most important influence on the penetration of an electrostatic field through the atmosphere. In altitude regions above 80 km the conductivity can no longer be taken as isotropic, since the influence of the rotation of the ionized particles around magnetic field lines becomes more important. The Ohm's law that relates electric field $\boldsymbol{E}$ and the current density $\boldsymbol{j}$, involves the conductivity tensor $\hat{\sigma}$. Let us split the vector $\boldsymbol{E}$ into field-aligned component $E_{\parallel}$ parallel to the magnetic field and the normal components $\boldsymbol{E}_{\perp}$,

$$j_{\parallel}=\sigma_{\parallel} E_{\parallel}, \tag{1}$$

$$\boldsymbol{j}_{\perp}=\sigma_P \boldsymbol{E}_{\perp}-\sigma_H [\boldsymbol{E}_{\perp}\times\boldsymbol{B}]/B, \tag{2}$$

where quantities σ_P, σ_H, $\sigma_{\parallel}$ are the Pedersen, Hall, and field-aligned conductivities (Hargreaves, 1979).

In the atmosphere below 80 km the conductivity tensor is isotropic one, so that $\sigma_H=0$, $\sigma_P=\sigma_{\parallel}=\sigma$. Values of the near Earth atmospheric conductivity σ are in the range 10^{-14} S/m to 10^{-13} S/m (Molchanov and Hayakawa, 1994). Huge variations are possible due to solar and geochemical influences (Prölss, 2003). Grimalsky et al. (2002) concluded that an increase of the near-Earth atmospheric conductivity leads to a modification of the electric environment of the ionosphere due to changed conditions for the electrostatic field penetration.

In this paper we are interested to study the possible influences of conductivity variations on the penetration of an electrostatic field through the atmosphere. Obviously, it is complicated to calculate regions where the conductivity is anisotropic. Thus it is necessary to obtain a proper upper boundary condition, which makes possible to estimate electrostatic fields at higher altitudes. In the section below, a model was obtained, where the atmospheric conductivity has the most important influence on the electrostatic field penetration.

2 Basic equations

Since we are interested in the steady state case the basic equations for the atmospheric electric field are the Faraday law, the charge conservation law and the Ohm's law

$$\nabla\times\boldsymbol{E} = 0 \tag{3}$$

$$\nabla \cdot \boldsymbol{j} = 0 \tag{4}$$

$$\boldsymbol{j} = \hat{\sigma} \boldsymbol{E}, \tag{5}$$

where the Ohm's law (Eqs. 1 and 2) is written in the short form. Because of (Eq. 3) the electric potential Φ can be introduced so that

$$\boldsymbol{E} = -\nabla \Phi. \tag{6}$$

Then the system of the equations (Eqs. 3–5) is reduced to the equation

$$-\nabla \cdot \left(\hat{\sigma} \cdot \nabla \Phi \right) = 0, \tag{7}$$

that would be the Laplace equation if the conductivity tensor $\hat{\sigma}$ is isotropic and constant.

3 Conductivity

Clearly one can see from Eq. (7) that the conductivity tensor $\hat{\sigma}$ takes a major part in our investigations. The conductivity is approximately isotropic in the atmosphere. It is regarded here as altitude range $0 \leq z \leq z_{\mathrm{up}}$, where z_{up}=80 km is the upper altitude range. The height distributions of the atmospheric conductivity can be approximated with an exponential function

$$\sigma(z) = \bar{\sigma} \exp(z/h), \tag{8}$$

where the conductivity only depends on an initial value $\bar{\sigma}$ and on the conductivity scale-height h.

In accordance with (Handbook of Geophysics, 1960) the typical values are $\bar{\sigma}=10^{-13}$ S/m, h=6 km for the main part of the atmosphere and $\bar{\sigma}=3 \cdot 10^{-14}$ S/m, h=3 km for the region near the ground. We mainly use the first set of the parameters and describe possible differences in the results due to this choice. Of course more detailed approximation than Eq. (8) can be used to present real conductivity distribution. However numerical solution of differential equations is necessary in such a model with no principal results in comparison with this simplified model, that permits to get the solutions analytically.

4 Model geometry

The geometry of the model is shown in Fig. 1. The origin of the coordinate system is exactly at the epicenter, the y-axis is directed along the fault and the x-axis is directed perpendicular to the fault. The z-axis is directed upward, from the ground to the ionosphere. The distribution only depends on the distance perpendicular to the tectonic fault x, but along the fault y the field is considered to be not variable. This simple approach is consistent with earlier work (Pulinets et al., 1998). As a tectonic fault is elongated, and some hundreds of kilometers long, one can also assume an elongated electrostatic field distribution on the Earth's surface. So we analyze the two-dimensional model in which no parameter depends on y. In such a model the equation (Eq. 7) has the form

$$-\frac{\partial}{\partial x}\left[\sigma(z)\frac{\partial}{\partial x}\Phi(x,z)\right] - \frac{\partial}{\partial z}\left[\sigma(z)\frac{\partial}{\partial z}\Phi(x,z)\right] = 0. \tag{9}$$

In our model the atmosphere is considered to be a horizontal layer between ground and some height z_{up}.

The general solution of this equation in such a domain can be obtained by separation of variables, i.e. superposition of exponential functions. To solve the differential equation, we need a lower and upper boundary conditions.

4.1 Lower boundary condition

As the lower boundary condition, the vertical component of the electric field on the Earth's surface is given

$$-\frac{\partial}{\partial z}\Phi(x,z)\,|_{z=0} = E_0(x). \tag{10}$$

The model distribution for the vertical electrostatic field can be written as (see Fig. 1):

$$E_0(x) = -\bar{E}_0(1+\cos(x\pi/a))/2, \qquad |x|<a. \tag{11}$$

where a indicates the size of the affected area on the Earth's surface, so that $E_0(x)=0$ outsides, and $\bar{E}_0$ is the maximal value of the electrostatic field at z=0 km. Quantity a can be interpreted as the earthquake preparation area. Negative vertical electrostatic fields on the ground means an increase of the fair weather electric field of the atmosphere. These values are in agreement with estimations of the electrostatic source in connection with an earthquake preparation process (Mikhailov et al., 2007; Pulinets and Boyarchuk, 2004). In our model $\bar{E}_0$=100 V/m and a=200 km were chosen. This value of a makes the function (Eq. 11) close to $-\bar{E}_0/\cosh(2x/c)$, that was used in the mentioned models with c=150 km. We opt for the function (Eq. 11) because it is equal to zero outside the domain of interest and stays smooth.

4.2 Upper boundary condition

The most significant results concerning the penetration of an electrostatic field into the ionosphere are related to the upper boundary condition (Grimalsky et al., 2003).

In our model the ionosphere is considered to be a horizontally stratified in the height more than some z_{up} above ground. It could be shown that because of the high field-aligned conductivity in the ionosphere our model of the ionospheric electric field is not sensitive to the value of z_{up}. We choose z_{up}=80 km. Our test calculations show no significant change if z_{up} is chosen in the range 80–90 km.

The inclination of geomagnetic field lines is assumed to be I=90°, which means vertical magnetic field lines that is nearly fulfilled in polar regions.

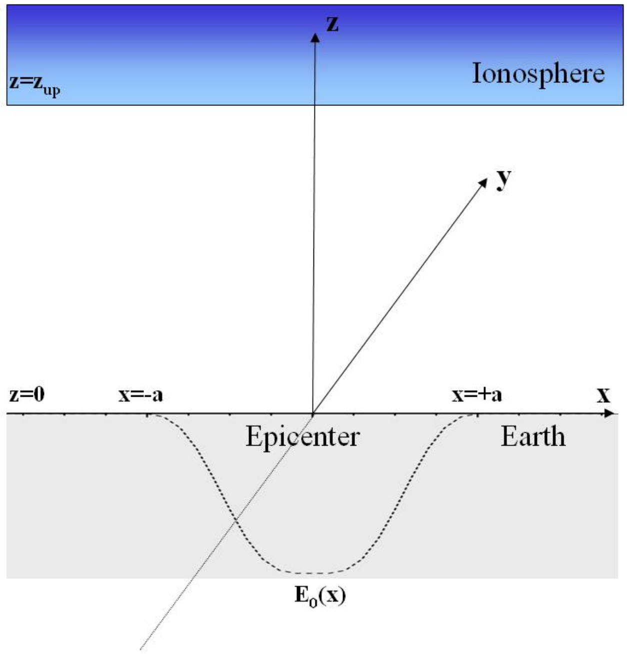

Fig. 1. Geometry of the model where the origin of the coordinate system is at the epicenter, and the x- and y-axis are perpendicular and along the fault, respectively.

The boundary $z=z_{\rm up}$ separates the region below it with isotropic finite conductivity, from the region above it with nearly infinite field-aligned conductivity. Below $z_{\rm up}$, the value of the conductivity increases by many orders of magnitude with increasing altitude. Above $z_{\rm up}$, the conductivity along geomagnetic field is considered to be huge (practically infinite). It means that the magnetic field lines are equipotential and $\boldsymbol{E}_\perp$ is independent of the height for $z>z_{\rm up}$. Therefore the Ohm's law (Eq. 2) can be integrated over z

$$\boldsymbol{J}=\int_{z_{\rm up}}^{\infty} \boldsymbol{j}_\perp dz=\begin{pmatrix}\Sigma_P & -\Sigma_H\\ \Sigma_H & \Sigma_P\end{pmatrix}\begin{pmatrix}E_x\\ E_y\end{pmatrix}, \tag{12}$$

where

$$\Sigma_P=\int_{z_{\rm up}}^{\infty}\sigma_P dz, \qquad \Sigma_H=\int_{z_{\rm up}}^{\infty}\sigma_H dz,$$

which are referred to as Pedersen – Σ_P – and Hall conductances – Σ_H – (Hargreaves, 1979). Since j_z from the atmosphere at $z=z_{\rm up}$ is closed with this $\boldsymbol{J}$, the charge conservation law means

$$\nabla \boldsymbol{J}=j_z\Big|_{z=z_{\rm up}}. \tag{13}$$

Using the Ohm's law in the atmosphere with scalar conductivity σ this equation can be written as the upper boundary condition for the equation (Eq. 9)

$$\left\{-\frac{\partial}{\partial x}(\Sigma_P\frac{\partial\Phi}{\partial x})+\sigma(z_{\rm up})\frac{\partial\Phi}{\partial z}\right\}\Big|_{z=z_{\rm up}}=0, \tag{14}$$

where the derivatives over y are omitted because no function depends on y. Moreover we use only constant Σ_P since the horizontal scale of interest is much less than the horizontal scale of the ionosphere.

5 Model calculation

To study the influence of ionospheric conductivity variations on the electrostatic field propagation through the atmosphere we use typical values of the ground value of the conductivity $\bar\sigma$ and the parameter h, and consider different values of Σ_P. The integrated conductivity Σ_P is assumed to be Σ_P=10 S in day-time (and in auroral zone) and Σ_P=0.1 S in night-time.

The boundary value problem (Eqs. 9, 10 and 14) aught to be solved in the two-dimensional domain $0<z<z_{\rm up}$, that is infinite in x direction. We can simplify the problem by addition some sources at large distances $b\gg a$ in such a manner that the solution of the original problem is not disturbed in the domain of interest, $|x|<2a$ for example. Namely we add

$$\bar E_0(1+\cos((x-b)\pi/a))/2,\ |x-b|<a,$$

and continue this function to the whole x-axis with period $2b$. The large parameter $b\gg a$ is chosen by test calculations so that such a modification of Eq. (11) has no influence on the results in the domain of interest $|x|<2a$.

After that we have the boundary value problem (Eqs. 9, 10 and 14) with additional condition of periodicity

$$\Phi(x+2b,z)=\Phi(x,z). \tag{15}$$

It is much more simple to deal with periodical functions since such a function can be presented with the Fourier Series, while the Fourier Integral is necessary (Korn and Korn, 1968) to present a function that is defined at the infinite axe and equals zero outside of some finite domain, that is $|x|<a$ for the original function $E_0(x)$ (Eq. 11).

Such a modification of the problem can be described by other words in the manner that is usual for numerical methods. The boundary value problem (Eqs. 9, 10 and 14) has a particular solution $\Phi(x,z)=\alpha x+\beta$ with arbitrary constants α, β. It can be used as the asymptotic at $x\to\infty$ and it means that $\Phi(x,z)$ is constant at vertical lines, when $x\to\infty$.
To avoid infinite domain it is possible to chose some large parameter b and approximately use this condition at $x=b/2$:

$$\Phi(b/2,z)=0. \tag{16}$$

The zero value is of no matter since any constant can be added to the potential. Because the solution is a symmetrical one with respect to x=0 line and Eq. (16) we also have

$$\Phi(-b/2,z)=0. \tag{17}$$

It is usual to use the boundary value problem with these additional conditions (Eqs. 16 and 17) instead of the original one.

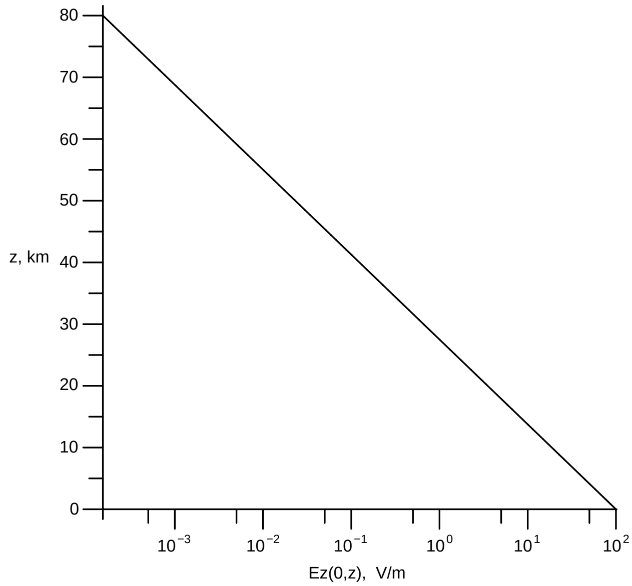

Fig. 2. The height distribution of the vertical electric field $E_z(0, z)$ above the point x=0.

Its solution is close to the solution of the original problem when $b\to\infty$. The conditions (Eqs. 16 and 17) permit to continue the function $\Phi(x, z)$ antisymmetrically $\Phi(b-x, z)=-\Phi(x, z)$ and to get a periodical function with $2b$ period as in the previous formula (Eq. 15).

The new function $E_1(x)$ equals to $E_0(x)$ (Eq. 11) in the interval $|x|<b-a$ and in contrast with $E_0(x)$ it can be presented as

$$E_1(x)=\sum_{n=0}^{\infty} f_n \cos(k_n x), \tag{18}$$

where

$$k_n=(2n-1)\pi/b. \tag{19}$$

The terms with even values $2n$ as well as all terms with $\sin(kx)$ are absent because the function $E_1(x)$ is antisymmetrical in respect of $x=b/2$ and symmetrical in respect of x=0.

The Fourier coefficients are equal

$$f_n=\tfrac{1}{b}\int_0^{2b} E_1(x)\cos(k_n x)dx.$$

Because of $E_1(x)$ symmetry and Eq. (16)

$$f_n=\tfrac{4}{b}\int_0^{b/2} E_1(x)\cos(k_n x)dx.$$

The interval of integration may be decreased to $0<x<a$ since $E_1(x)$=0 at $a<x<b/2$. Because of that $E_1(x)=E_0(x)$ at $0<x<a$ the formula (Eq. 11) can be used and the integral can be calculated analytically

$$\begin{aligned} f_n &= \frac{2}{b}\int_0^a (1+\cos(x\pi/a))\cos(k_n x)dx \\ &= \frac{2\sin(k_n a)}{bk_n((k_n a/\pi)^2-1)}\bar{E}_0. \end{aligned} \tag{20}$$

If $k_n a=\pi$, that means $2n_0-1=b/a$, the denominator equals zero, but the numerator also equals zero and this $f_n=a/b$. It can not occur if b/a is not integer. The coefficients f_n are large for n close to this $n_0=(b/a+1)/2$ and decrease as $1/n^3$ for $n\to\infty$.

The general solution of equation (Eq. 9) can be found due to separation of variables and is a superposition of exponential functions, depending on x and z separately

$$\Phi(x, z)=\sum_{0}^{\infty} cos(k_n x)\left(A_n e^{\lambda_n z}+B_n e^{\Lambda_n z}\right), \tag{21}$$

where

$$\begin{aligned} \lambda_n &= -\frac{1}{2h}+\sqrt{\left(\frac{1}{2h}\right)^2+k^2}, \\ \Lambda_n &= -\frac{1}{2h}-\sqrt{\left(\frac{1}{2h}\right)^2+k^2}. \end{aligned} \tag{22}$$

The coefficients A_n and B_n can be derived from the boundary conditions given in Eqs. (10) and (14).

We use the presentation (Eq.15) for $E_0(x)$ since $E_1(x)=E_0(x)$ for $|x|<b-a$ and the parameter b is large enough and it does not disturb the solution.

With the constitutive relation,

$$\alpha_n=\frac{\Sigma_P k^2+\bar{\sigma}\exp[z_{\rm up}/h]\lambda_n}{\Sigma_P k^2+\bar{\sigma}\exp[z_{\rm up}/h]\Lambda_n}e^{(\lambda_n-\Lambda_n)z_{\rm up}}, \tag{23}$$

the coefficients are

$$\begin{aligned} A_n &= f_n(\lambda_n-\Lambda_n\alpha)^{-1}, \\ B_n &= -\alpha A_n. \end{aligned} \tag{24}$$

The components of the electric field in the atmosphere can be deduced from Eq. (6)

$$E_x(x, z)=-\frac{\partial}{\partial x}\Phi(x, z) \tag{25}$$

$$E_z(x, z)=-\frac{\partial}{\partial z}\Phi(x, z), \tag{26}$$

where the potential $\Phi(x, z)$ is calculated by the formula (Eq. 21). The third component $E_y(x, z)$=0 since there is no variation along the y coordinate.

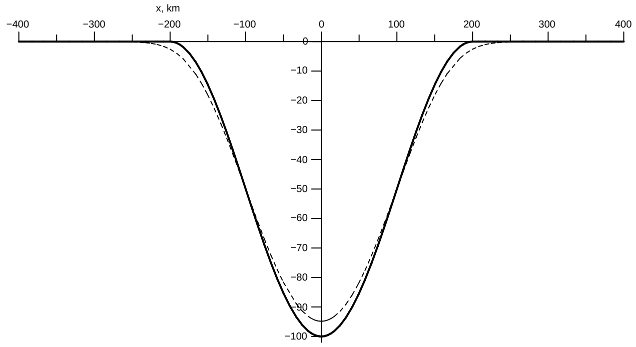

Fig. 3. Electric field at the ground $E_z(x, 0)$ - solid line, and at the bottom of the ionosphere $E_z(x, z_{\mathrm{up}})$ - dashed line. The maximal values are 100 V/m and 9 μV/m, respectively.

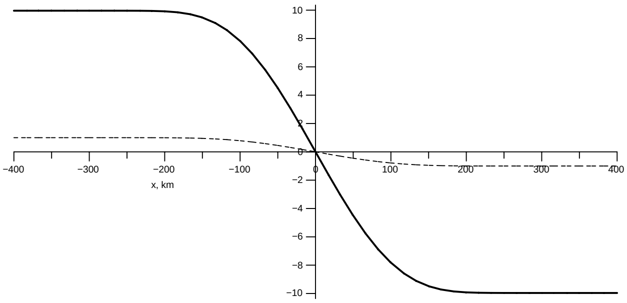

Fig. 4. Horizontal electric field S $E_x(x, z_{\mathrm{up}})$, μV/m in the night-time ionosphere with Σ_P=0.1 S - solid line, and in the ionosphere with Σ_P=1 S - dashed line.

6 Summary of the main results

The results of the electric field calculations are presented in Fig. 2. It presents the height distribution of the vertical component of the electric field at the line x=0. This graph is hardly distinguished from the line

$$E_z(0, z)=E_z(0, 0)\sigma(0)/\sigma(z), \tag{27}$$

which corresponds to the fact that the vertical electric current density does not vary with height.

The shape of horizontal cross-section of $E_z(x, z)$ is almost independent of the height as it can be seen in Fig. 3. The $E_z(x, z)$ distributions at the ground and at the upper boundary of the atmosphere are plotted in such scales that these two lines would be identical if Eq. (24) is exactly valid. For this purpose the dashed line presents the vertical electric field in the ionosphere $E_z(x, z_{\mathrm{up}})$ multiplied by $\exp(z_{\mathrm{up}}/h)$. So the maximal values are 100 V/m and 9μV/m, respectively.

Figures 2 and 3 show that the vertical component of the current density almost does not vary with height. The domain $|x|<a$ of nonzero j_z at the ground slightly increases up to the ionosphere. The total current per Δy=1 m

$$J_z=\int_{-2a}^{2a} j_z dx$$

does not depend on z in view of the charge conservation law. Here we regard $2a$ as a large distance, but less than $b/2$ to exclude the influence of the added periodically current sources at the ground. So this current can be calculated using the Ohm's law and given values of conductivity $\bar{\sigma}$ at the ground and $E_z(x, 0)$ (Eq. 11)

$$J_z = \int_{-a}^{a} j_z dx = \int_{-a}^{a} \sigma(0) E_z(x, 0) dx$$
$$= -\bar{\sigma}\bar{E}_0 a = -2\mu A/m.$$

with values of the parameters $\bar{E}_0$=100 V/m, a=200 km and $\bar{\sigma}$=10^{-13} S/m, which are chosen in Sects. 3 and 4.1, respectively. This current J_z goes to the ground through atmosphere from the ionosphere. In accordance with charge conservation law the same current must go along the ionosphere from its far regions, $J_z/2$ from both infinities because of the symmetry. Horizontal electric field is necessary for such currents

$$E_x = \pm \frac{1}{2} J_z/\Sigma_P = \pm \frac{\bar{\sigma}\bar{E}_0 a}{2\Sigma_P}. \tag{28}$$

It is equal to $\mp 1\,\mu$V/m for $x \gg a$ and $x << -a$ if Σ_P=1 S. The typical values of Σ_P vary from 0.1 S in the night-time ionosphere till 10 S in the day-time ionosphere and in the auroral zone.

These limit values, i.e. $\mp 10\,\mu$V/m, in the night-time ionosphere are shown in Fig. 4 for $|x|>200$ km. The calculated $E_x(x)$ presented in this figure for the upper boundary of the atmosphere stays the same in the ionosphere in the frame of our model because of the large field-aligned conductivity in the ionosphere.

The electric field in the ionosphere is not more than 10 μV/m, since other values of Σ_P give decrease of E_x. It can be seen in Fig. 4 where $E_x(x)$ for Σ_P=1 S is shown by dashed line. The day-time $E_x(x)$ distribution has almost the same shape, but it is invisible in this scale because its maximum equals 0.1 μV/m.

The electric fields of these magnitudes can not be observed in the ionosphere because much larger fields, definitely more than 1 μV/m are always present there.

Figure 5 gives general view of the electric potential in the atmosphere. Because of the simple properties of the electric field described above, it is possible to obtain analytical solution with a rather good precision.
As the results of Eqs. (6), (8) and (24),

$$\Phi(x, z) = -\int_z^{z_{\mathrm{up}}} |E_0(x)| \exp(-z/h) dz$$
$$= |E_0(x)| h \left(\exp(-z/h) - \exp(-z_{\mathrm{up}}/h)\right),$$

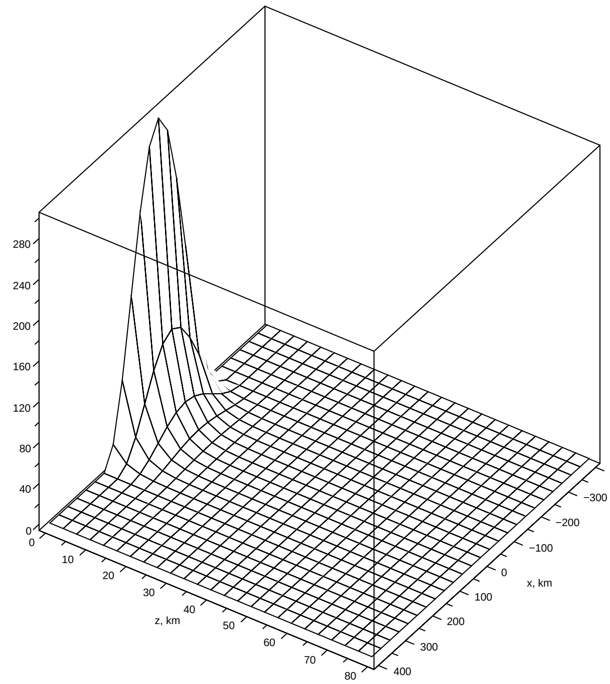

Fig. 5. Electric potential in atmosphere $\Phi(x, z)$ kV.

if we approximately consider Φ=0 in the ionosphere. Since the second term is small far from the ground, approximately

$$\Phi(x, z) = |E_0(x)| h \exp(-z/h).$$

The maximal value equals $E_0(x)h$=600 kV. This value must be decreased if we take into account specific $\sigma(z)$ behavior near the ground where h=3 km gives better approximation (Handbook of Geophysics, 1960). Then the maximal potential difference between ground and ionosphere becomes about 300 kV. Such an electric potential distribution is presented in Fig. 5. It almost does not depend on $\sigma(z)$ distribution above z=5 km.

The described simple properties of $\boldsymbol{E}$ and Φ space distributions are mainly due to large horizontal scale $a \gg h$. If the region of the electric field generator near the analyzed earthquake becomes less, the ionospheric electric field is proportionally decreased in our model in accordance with the estimations (Eq. 25). So 10 μV/m can be regarded as the upper limit of possible electric field penetrated into the ionosphere.

7 Discussion and conclusion

The details of $E_x(x, z)$ distribution are defined by the solution for the boundary value problem (Eqs. 9, 10 and 14), but the scale of the penetrating field can be calculated by the formula (Eq. 25) in a wide range of parameters which characterize the atmospheric and ionospheric conductivities while the horizontal scale of the process a is large enough.

This conclusion and estimations by the formula (Eq. 25) contradict the former calculations (Pulinets et al., 1998), where the maximum of the horizontal electrostatic field penetration is in the mV/m range.

The electric field at the ground can not be much larger than 100 V/m, that is used both here and in former models, since it gives a few hundreds kV potential difference between ionosphere and ground. So, the only way to get large penetrated electric field may be due to atmospheric conductivity near the ground hundred times increased in comparison with usual conditions.

Because the conductivity along geomagnetic field lines is much greater than the conductivities perpendicular to the field lines, and because of the assumption, that geomagnetic field lines are parallel in the ionosphere, the electric field intensity will not change significantly in higher altitudes. This is taken into account in the effective upper boundary condition (Eq. 14). Thus, the electrostatic field at the altitude z_{up}=80 km can be used to calculate effects in higher regions.

The assumption of vertical geomagnetic field lines (I=90°) is almost fulfilled in polar regions. In the frame of satellite missions, data generally is recorded at latitudes below a specific region. In the case of DEMETER, observations are performed at latitudes less than 65° on both hemispheres. This means, the model calculation obtained here must be expanded to oblique geomagnetic field lines to improve the results.

The designed model suppose vertical magnetic field, that is not valid in middle and low latitudes. It is of matter only for the value of the conductance of the ionosphere, since the atmospheric conductivity is a scalar that is independent of magnetic field. If we take the inclination into account, the conductance tensor with parameters Σ_P, Σ_H (Eq. 12) must be changed with tensor with coefficients Σ_{xx}, $\Sigma_{xy}=-\Sigma_{yx}$, Σ_{yy} (Hargreaves, 1979). Since these parameters are independent of x, y the terms with $\Sigma_{xy}=-\Sigma_{yx}$ do not appear in the upper condition (Eq. 14) after such a modification as well as Σ_H is not present in (Eq. 14):

$$\left\{-\frac{\partial}{\partial x}\left(\Sigma_{xx}\frac{\partial \Phi}{\partial x}\right)+\sigma(z_{\mathrm{up}})\frac{\partial \Phi}{\partial z}\right\}\Big|_{z=z_{\mathrm{up}}}=0. \quad (29)$$

If we exclude for simplicity a narrow region near the geomagnetic equator, then $\Sigma_{xx}=\Sigma_P/\cos 2\chi$, $\Sigma_{yy}=\Sigma_P$, where χ is the angle between vertical and magnetic field, that is in x, z plane (Hargreaves, 1979). Of cause $\Sigma_{xx}=\Sigma_P$ if magnetic field is inclined in y, z plane and some average value would be in general case.
Anyway, the conductance Σ_{xx} can only be increased in comparison with Σ_P. Hence the magnitude of the electric field in the ionosphere is smaller if we take the inclination into account.

From our investigations, it comes that the electric field penetration is approximately proportional to the atmospheric conductivity near the ground and inverse proportional to the integral ionospheric Pedersen conductivity. Also this penetrated electric field is a hundred times larger during night-time in comparison with day-time one, and its penetration of electrostatic fields depends on various characteristics of the conductivity distributions. However our estimations show that the field penetration is damped and no seismic precursor may be seen in the ionosphere.

Future investigation, the height distribution and the dynamic behavior of the atmospheric conductivity must be more better known, especially its increase near the ground during seismic events.

Acknowledgements. This work is supported by grant 07-05-00135 from the Russian Foundation for Basic Research and by the Programs 16.3 and 2.16 of the Russian Academy of Sciences. Further support is due to the Austrian "Fonds zur Förderung der wissenschaftlichen Forschung" under project P20145-N16. We acknowledge support by the Austrian Academy of Sciences, "Verwaltungstelle für Auslandsbeziehungen", and the Russian Academy of Sciences. Part of this research was done during academic visits of V. V.'Denisenko to the Space Research Institute of the Austrian Academy of Sciences in Graz as well as during an academic visit of H. K. Biernat to the Institute of Computational Modelling of the Russian Academy of Sciences in Krasnoyarsk.

Edited by: M. Contadakis

Reviewed by: J.-J. Berthelier and another anonymous referee

References

Baginski, M. E., Hale, L. C., and Olivero, J. J.: Lightning-related fields in the ionosphere, Geophys. Res. Lett., 15, 764–767, 1988.

Boyarchuk, K. A., Lomonosov, A. M., Pulinets, S. A., and Hegai, V. V.: Variability of Earth's atmospheric electric field and ion-aerosols kinetics in the troposphere, Stud. Geophys. Geod., 42, 197–210, 1998.

Depuev, V. and Zelenova, T.: Electron density profile changes in a pre-earthquake period, Adv. Space Res., 18(6), 115–118, 1996.

Dobrovolsky, I. P., Zubkov, S. I., and Miachkin, V. I: Estimation of the size of earthquake preparation zones, Pure Appl. Geophys., 117, 1025–1044, 1979.

Gershenzon, N. and Bambakidis, G.: Modeling of seismo-electromagnetic phenomena, Russian Journal of Earth Science, 3, 247–275, 2001.

Gershenzon, N. I., Gokhberg, M. B., and Yunga, S. L.: On the electromagnetic field of an earthquake focus, Phys. Earth Planet. In., 77, 13, 1993.

Gokhberg, M. B., Gershenzon, N. I., Gufel'd, I. L., Kustov, A. V., Liperovskiy, V. A., and Khusameddimov, S. S.: Possible effects of the action of electric fields of seismic origin on the ionosphere, Geomagn. Aeronomy+, 24, 183, 1984.

Gokhberg, M. B., Gufel'd, I. L., Gershenzon, N. I., and Pilipenko, V. A.: Electromagnetic effects during rupture of the Earth's crust, Izvestiya Russian Academy of Sciences, Physics of the Solid Earth, 21, 52, 1985.

Gokhberg, M. B., Pilipenko, V. A., and Pokhotelov, O. A.: Seismic precursors in the ionosphere, Izvestiya Russian Academy of Sciences, Physics of the Solid Earth, 19(10), 762–765, 1983.

Grimalsky, V. V., Hayakawa, M., Ivchenko, V. N., Rapoport, Y. G., and Zadorozhnii, V. I.: Penetration of an electrostatic field from the lithosphere into the ionosphere and its effect on the D-region before earthquakes, J. Atmos. Sol.-Terr. Phys., 65, 391–407, 2003.

Grimalsky, V. V., Koshevaya, S., Perez-Enriquez, R., and Kotsarenko, A.: Electrostatic field variations in the lower ionosphere due to the change of near–earth atmosphere conductivity – 3D modeling, 27th General Assembly of the International Union of Radio Science, Maastricht, Netherlands, 17–24 August 2002.

Handbook of Geophysics, The Macmillan Company, New York, 1960.

Hargreaves, J. K.: The upper atmosphere and Solar-Terrestrial relations, Van Nostrand Reinold Co. Ltd, NY, 1979.

James, H. G.: The ELF Spectrum of Artificially Modulated D/E – Region Conductivity, J. Atmos. Terr. Phys., 47, 1129–1142, 1985.

Kamra, A. K. and Ravichandran, M.: On the assumption of the Earth's surface as a perfect conductor in atmospheric electricity, J. Geophys. Res., 98, 22 875–22 885, 1993.

Kelley, M. C. and Mozer, F. S.: A satellite survey of vector electric fields in the ionosphere at frequencies of 10 to 500 Hertz, 3. Low-frequency equatorial emissions and their relationship to ionospheric turbulence, J. Geophys. Res., 77, 4183, 1972.

Kelley, M. C., Livingston, R., and McCready, M.: Large amplitude thermospheric oscillations induced by an earthquake, Geophys. Res. Lett., 12, 577, 1985.

Khegay, V. V., Kim, V. P., and Illich-Svitych, P. V.: The formation of a cavity in the night–time midlatitude ionospheric E-region above a thundercloud, Planet. Space Sci., 38, 703–707, 1990.

Kim, V. P., Hegaj, V. V., and Illich-Switych, P. V.: On the possibility of a metallic ion layer forming in the E-region of the night midlatitude ionosphere before great earthquakes, Geomagn. Aeronomy+, 33, 658–662, 1994.

Kim, V. P. and Khegay, V. V.: The effect of an electric field on the nightside E region of the midlatitude ionosphere, Geomagn. Aeronomy+, 25, 717–718, 1985.

Kingsley, S. P.: On the possibilities for detecting radio emissions from earthquakes, Il Nuovo Cimento, 12, 117, 1989.

Kondo, G.: The variation of the atmospheric electric field at the time of earthquake, Memoirs of the Kakioka Magnetic Observatory, 13, 11–23, 1968.

Korn, G. A. and Korn, T. M.: Mathematical handbook, McGraw-Hill Book Company, New York, 1968.

Liu, J. Y., Chuo, Y. J., Shan, S. J., Tsai, Y. B., Chen, Y. I., Pulinets, S. A., and Yu, S. B.: Pre-earthquake ionospheric anomalies registered by continuous GPS TEC measurements, Ann. Geophys., 22, 1585–1593, 2004, http://www.ann-geophys.net/22/1585/2004/.

Ma, Z., Croskey, C. L., and Hale, L. C.: The electrodynamic responses of the atmosphere and ionosphere to the lightning discharge, J. Atmos. Terr. Phys., 60, 845–861, 1998.

Makino, M. and Ogawa, T.: Responces of atmospheric electric field and air-earth current to variations of conductivity profiles, J. Atmos. Terr. Phys., 46, 431–445, 1984.

Martynenko, S. I., Fuks, I. M., and Shubova, R. S.: Ionospheric electric-field influence on the parameters of VLF signals connected with nuclear accidents and earthquakes, J. Atmos. Electr., 16, 259–269, 1996.

Mastov, S. R. and Lasukov, V. V.: A theoretical model of generation of an electromagnetic signal in brittle failure, Izvestiya Russian Academy of Sciences, Physics of the Solid Earth, 25, 478, 1989.

Mikhailov, Y. M., Mokhailova, G. A., Kapustina, O. V., Buzevich, A. V., and Smirnov, S. E.: Atmospheric noise extremes in quasi-static electric field variation in the near ground atmosphere of Kamchatka, in Proceedings of the IV International Conference on Solar-Terrestrial Relations and Precursors of Earthquakes, Kamchatka, Russia, 14–17 August 2007.

Molchanov, O. A.: Transmission of electromagnetic fields from seismic sources to the upper ionosphere, Geomagn. Aeron.+, 31, 80–85, 1991.

Molchanov, O. A. and Hayakawa, M.: On the generation mechanism of ULF seismogenic electromagnetic emissions, Phys. Earth Planet. In., 105, 201–210, 1998.

Molchanov, O. A. and Hayakawa, M.: Generation of ULF electromagnetic emissions by microfracturing, Geophys. Res. Lett., 22, 3091–3094, 1995.

Molchanov, O.A:, Hayakawa, M.: Generation of ULF seismogenic electromagnetic emission: A natural consequence of microfracturing process, in: Electromagnetic phenomena related to earthquake prediction, edited by: Hayakawa, M. and Fujinawa, Y., Terra Scientific Publishing Company, Tokyo, 537–563, 1994.

Molchanov, O., Fedorov, E., Schekotov, A., Gordeev, E., Chebrov, V., Surkov, V., Rozhnoi, A., Andreevsky, S., Iudin, D., Yunga, S., Lutikov, A., Hayakawa, M., and Biagi, P. F.: Lithosphere-atmosphere-ionosphere coupling as governing mechanism for preseismic short-term events in atmosphere and ionosphere, Nat. Hazards Earth Syst. Sci., 4, 757–767, 2004, http://www.nat-hazards-earth-syst-sci.net/4/757/2004/.

Molchanov, O. A., Hayakawa, M., and Rafalsky, V. A.: Penetration characteristics of electromagnetic emissions from an underground seismic source into the atmosphere, ionosphere, and magnetosphere, J. Geophys. Res., 100, 1691–1712, 1995.

Nisbet, J. S.: A dynamic model of thundercloud electric field, J. Atmos. Terr. Phys., 40, 2855–2873, 1983.

Park, C. G. and Dejnakarintra, M.: Penetration of thundercloud electric fields into the ionosphere and magnetosphere, 1. Middle and auroral latitudes, J. Geophys. Res., 84, 960–964, 1973.

Parrot, M., Berthelier, J. J., Lebreton, J. P., Sauvaud, J. A., Santolik, O., and Blecki, J.: Examples of unusual ionospheric observations made by the DEMETER satellite over seismic regions, Phys. Chem. Earth, 31, 486–495, 2006.

Parrot, M.: Use of satellites to detect seismo-electromagnetic effects, Adv. Space Res., 15(11), 27–35, 1995.

Pierce, E. T.: Atmospheric electricity and earthquake prediction, Geophys. Res. Lett., 3, 185–188, 1976.

Pogorel'tsev, A. I.: Disturbances of electric and magnetic fields induced by the interaction of atmospheric waves with the ionospheric plasma, Geomagn. Aeronomy+, 29, 286–292, 1989 (in Russian).

Prölss, G.W.: Physik des erdnahen Weltraums, Eine Einführung, Berlin, Heidelberg, New, York, Springer, 2003.

Pulinets, S. A. and Boyarchuk, K.: Ionospheric precursors of earthquakes, Berlin, Heidelberg, New York, Springer, 2004.

Pulinets, S. A., Legen'ka, A. D., Gaivoronskaya, T. V., and Depuev, V. K.: Main phenomenological features of ionospheric precursors of strong earthquakes, J. Atmos. Sol.-Terr. Phy., 65, 1337–1347, 2003.

Pulinets, S. A., Boyarchuk, K. A., Hegai, V. V., and Karelin, A. V.: Conception and model of seismo-ionosphere-magnetosphere coupling, in SeismoElectromagnetics Lithosphere-Atmosphere-Ionosphere coupling, edited by: Hayakawa, M. and Molchanov, O. A., Terrapub, Tokyo, 353–361, 2002.

Pulinets, S. A., Boyarchuk, K. A., Hegai, V. V., Kim, V. P., and Lomonosov, A. M.: Quasielectrostatic model of atmosphere-thermosphere-ionosphere coupling, Adv. Space Res., 26, 1209–1218, 2000.

Pulinets, S. A., Hegai, V. V., Kim, V. P., and Depuev, V. K.: Unusual longitude modification of the night-time mid-latitude F2 region ionosphere in July 1980 over the array of tectonic faults in the Andes area: observations and interpretation, Geophys. Res. Lett., 25, 4133–4136, 1998.

Roble, R. G. and Hays, P. B.: A quasi-static model of global atmospheric electricity. II – Electrical coupling between the upper and the lower atmosphere, J. Geophys. Res., 84, 7247–7256, 1979.

Rodger, C. J., Thomson, N. R., and Dowden, R. L.: Testing the formulation of Park and Dejnakarintra to calculate thunderstorms dc electric fields, J. Geophys. Res., 103, 2171–2178, 1998.

Row, R. V.: Acoustic-gravity waves in the upper atmosphere due to a nuclear detonation and an earthquake, J. Geophys. Res., 72, 1599–1610, 1967.

Ruzhin, Y. Y., Depueva, A. K., and Gorduk, V. P.: Signature of atomic station at lower ionosphere as plasma anomalies of Es layer, Adv. Space Res., 15(11), 157–159, 1995.

Ruzhin, Y. Y. and Depueva, A. K.: Seismoprecursors in space as plasma and wave anomalies, J. Atmos. Electr., 16, 271–288, 1996.

Sharma, D. K., Rai, J., Chand, R., and Israil, M.: Effect of seismic activities on ion temperature in the F2 region of the ionosphere, Atmósfera, 19, 1–7, 2006.

Silina, A. S., Liperovskaya, E. V., Liperovsky, V. A., and Meister, C.-V.: Ionospheric phenomena before strong earthquakes, Nat. Hazards Earth Syst. Sci., 1, 113–118, 2001, http://www.nat-hazards-earth-syst-sci.net/1/113/2001/.

Sorokin, V. M., Yaschenko, A. K., Chmyrev, V. M., and Hayakawa, M.: DC electric field amplification in the mid-latitude ionosphere over seismically active faults, Nat. Hazards Earth Syst. Sci., 5, 661–666, 2005, http://www.nat-hazards-earth-syst-sci.net/5/661/2005/.

Sorokin, V. M., Chmyrev, V. M., and Yaschenko, A. K.: Electrodynamic model of the lower atmosphere and the ionosphere coupling, J. Atmos. Sol-Terr. Phy., 63, 1681–1691, 2001.

Sorokin, V. and Yaschenko, A.: Electric field disturbance in the Earth-ionosphere layer, Adv. Space Res., 26, 1219-1223, 2000.

Trakhtengerts, V. Y.: The generation of electric fields by aerosol particle flow in the middle atmosphere, J. Atmos. Terr. Phys., 56, 337–342, 1994.

Tzur, I. and Roble, R. G., The interaction of a dipolar thunderstorm with its global electrical environment, J. Geophys. Res., 90, 5989–5999, 1985.

Velinov P. I. and Tonev, P. T.: Modelling the penetration of thundercloud electric field into the ionosphere, J. Atmos. Terr. Phys., 57, 687–694, 1995.